Quality monitoring of Concrete 3D Printed elements using computer vision-based texture extraction technique

Shanmugaraj Senthilnathan[1] and Benny Raphael[2*]

[1,2]Civil Engineering Department, Indian Institute of Technology Madras, India
[1]ce20d005@smail.iitm.ac.in, [2*]benny@civil.iitm.ac.in

Abstract –
Concrete 3D Printing (3DP) has the potential to reduce construction time and the usage of labor and material in the construction industry. However, many parameters are found to influence the output of 3DP, and consequently, the variations in the quality of output are high. To fully realize the advantages of 3DP and to develop it into a technology for large-scale construction, a focus on quality monitoring and control is required. The workability of concrete is found to reduce with time, impacting the extrudability and buildability properties. This can be seen in 3DP elements, where the bottom layers are found to have a smooth textural finish while the top layers have cracks, voids, and defects. To quantify the extrudability changes in the concrete, a new computer-vision-based methodology is proposed in this paper using a modified Histogram of Oriented Gradients (HOG) texture extraction method. Different levels of texture variations are extracted to quantify both minor and major textural changes. Weighted texture and normalized weighted texture metrics are introduced to have a combined single measure for minor and major textural variations. Further, a temporal textural change study is proposed to indirectly assess the buildability properties of concrete 3DP. This paper contributes to developing a non-intrusive autonomous quality monitoring and assessment technique for concrete 3D printed elements.

Keywords –
Concrete 3D printing; Computer Vision; Histogram of Oriented Gradients; Extrudability; Quality monitoring

1 Introduction and background

Concrete 3D printing (3DP) is an emerging free-form-based digital construction technology that has the potential to improve automation in the construction industry. 3DP increases productivity by reducing construction time while also reducing material and labor usage. Though there are many advantages, employing the technology on a larger scale requires maturity in terms of repeatability and quality control [1]. But the number of studies on quality control in concrete 3DP is limited, and many industry experts consider it a critical topic [2].

Since concrete 3DP depends on many input parameters, the quality of printed extrudates varies drastically [3]. Effective quality control systems help to avoid re-work and material wastage. The output quality of the concrete 3DP elements varies with the reduction in the material's workability and moisture content. The bottom layers are seen to have a smooth surface texture finish, and the top layers have a more granular finish, ultimately leading to voids/discontinuities. The changes in workability are found to affect the extrudability and buildability properties of concrete [4]. Extrudability is the ability of the concrete to pass with a high shear through a nozzle and maintain the liquid properties. Buildability is the ability of concrete to maintain its shape without much deformation under the influence of the weights of successive layers. There have been studies that use mechanical tests to quantify workability over time [5], but they cannot be used for real-time monitoring [6].

Computer vision (CV) has gained significant importance in additive manufacturing[7] and slowly getting traction in concrete 3DP [8][9]. Hence there are very few studies in concrete 3DP using CV for quality assessment and using it for real-time feedback to control the quality of 3D printing.

This study proposes the use of images and videos of 3D printed elements to evaluate the surface textural variations. CV-based texture extraction helps to obtain surface textural variations within each printed layer image to detect defects like voids and discontinuities. It is a continuation of the previous work [6], which utilized a different two-bin Local Binary Pattern (LBP) algorithm that only captured texture variation in the horizontal direction. A novel approach to capture texture in three directions with a method to categorize minor and major textural variations is developed in this study to assess the quality of the printed layers. Also, a temporal textural variation study is introduced to assess the buildability properties.

1.1 Objective

The main objective of this study is to develop a non-intrusive autonomous quality monitoring and assessment methodology using a CV-based texture extraction method.

1.2 Methodology

An overview of the methodology is shown in Figure 1. It involves collecting images or videos of 3D-printed layers during the printing process. Pre-processing is done to crop the individual layers into separate images, which are used in textural analysis to extract the variations within each layer. A novel method is proposed to capture both minor and major textural variations.

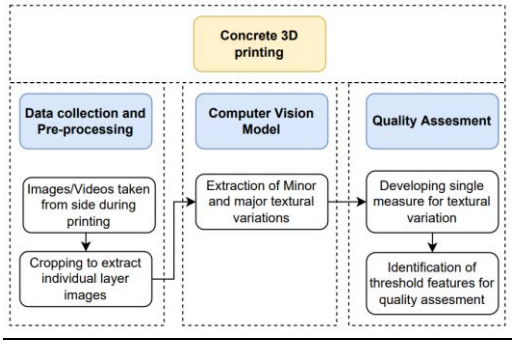

Figure 1 - Methodology of quality assessment using computer vision

A single metric is developed to capture all the minor and major textural variations. And a threshold for the metric is identified for assessing the quality of the printed layers.

2 Materials and Methods

2.1 Materials used

For this study, sample 3D printed elements were printed with a recently developed Limestone Calcined Clay (LC2) mix composed of OPC cement and Limestone Calcined Clay as the binder materials [10]. The aggregate used was 4.75mm size Manufactured Sand. Super-plasticizers and powder-based Viscosity Modifying Admixtures (VMA) were used to achieve optimum rheological properties of the mix to print.

A gantry-based robotic printer is used in this study. For evaluating the newly developed methodology, two specimens were used. One circular cross-section element was printed for a height of 1000 mm. Another circular 3D-printed element of height 700 mm was printed with a chemical-based super-plasticizer. Since it was a chemical-based super-plasticizer, there were many voids, and the printing was stopped at 700 mm as it may lead to the clogging of pipes.

2.2 Image Data Collection and Pre-processing

Since the current study is focused on extracting the texture variations in all the layers, image/video data is collected by keeping a camera perpendicular to the printed element. The camera is positioned 1.5 m horizontally from the printed elements, such that all the side layers are visible in a single shot of the 3D-printed element. Since a single picture containing all the layers was used for the analysis, the influence of differential illumination on different images is avoided.

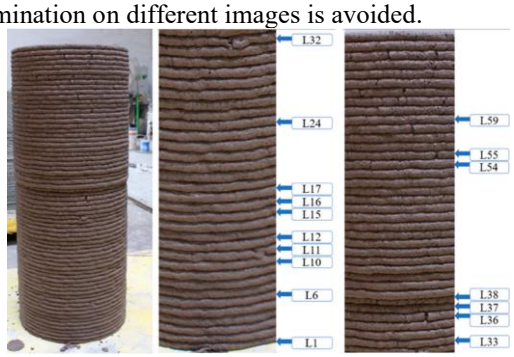

Figure 2 - Printed element A (left), bottom section of Element A taken for analysis - Section A1 (middle), Top section of Element B taken for analysis - Section A2 (right)

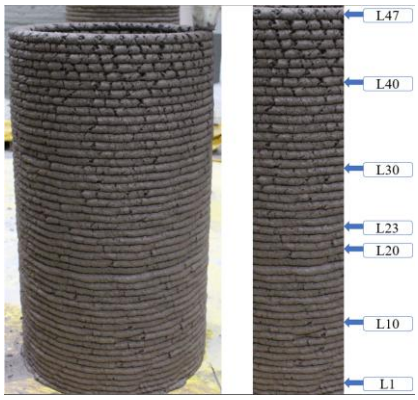

Figure 3 - Printed Element B (left), Section considered for analysis and the layer designations of Element B (right)

The camera used in the study is a Canon EOS 1300D DSLR camera with an 18 MP resolution. Since the printed elements are of circular cross-sections, images/videos taken from the sides will have the impact of curvature. The central one-third of the image is used in this study to avoid the curvature effects on the analysis.

The individual layers of the printed element are cropped to create the input images for analysis. The individual layer elements are designated as L1 for the bottom layer and numbered sequentially for the top layers. The two printed elements-Element A and B, and their layer designations are given in Figure 2 and Figure 3,

respectively. The cropping of individual layers was done manually in this study, but it can be automated using computer vision techniques like image segmentation. It is a part of ongoing research and is proposed as a part of future work.

2.3 Texture extraction – Histogram of Oriented Gradients (HOG)

The layer images were analyzed using a texture extraction algorithm written in Python language. Multiple texture extraction algorithms were evaluated for their capability to identify quality defects in 3DP concrete specimens. A custom-designed version of the Histogram of Oriented Gradients (HOG) approach was found to give the best results.

The Histogram of Oriented Gradients (HOG) was first conceptualized in 1986. It is a popular feature extractor that can extract useful information from the given image and eliminate unwanted information. HOG uses the gradients of pixel values in the images [11]. The gradient measures the pixel intensity variation in a particular direction. The gradient can be computed in one or many directions.

In this study, a new version of the HOG feature extractor is designed to extract gradients in three different directions using masks, as shown in Figure 4, namely, Horizontal, Vertical, and Diagonal masks. The masks were designed based on Robert's filter to detect the edges in images. Application of each mask at a pixel position involves taking an inner product of the matrix with the corresponding pixel values in the neighborhood of the pixel position.

Horizontal Mask		Vertical Mask		Diagonal Mask	
-1	0	-1	1	-1	0
1	0	0	0	0	1

Figure 4 - Gradient masks used for texture extraction

These masks are convoluted across the input images; the inner product is calculated at each pixel position. To consider both minor and major texture variations, a range of thresholds is used to calculate the number of pixels that have large gradients. A window size of 4 image pixels (2x2) is chosen for the study.

The individual pixel windows are convoluted with the horizontal, vertical, and diagonal masks to get the output gradients. The output of the HOG operator is taken as the number of pixels having gradient changes in any one of the directions after converting the images into grayscale.

The HOG algorithm developed in this work is different from the conventional HOG algorithm in the following aspects: the histogram is computed using the count of pixels having gradient greater than different threshold values; that is, it computes the gradient in horizontal, vertical, and inclined directions and counts the number of pixels where the gradient exceeds the threshold.

Since the count of the HOG gradient variations gives the textural variations within the printed element, the output of the HOG operator shall be called as texture in this study.

2.4 Weighted mean calculation

From the HOG analysis, different outputs are obtained for a single-layer image for different threshold values. The smaller threshold outputs will capture all the minor gradient changes, and the larger threshold captures only the major textural variations like voids and discontinuities.

The voids/discontinuities in the printed layers contribute to the major textural changes. Hence maximum weightage is given for large threshold values; that is, the threshold of 128 is given the maximum weightage and the threshold of 4 the minimum. Then the weighted mean is computed for each of the "i" threshold values, as per the following equation,

Weighted mean of the image = $\sum(w_i * x_i) / \sum(w_i)$

Where, w_i – the weight given for the threshold value "i", x_i – HOG output of the image for the threshold value "i". The weighted mean is computed for each of the individual layer images and then tabulated. The weighted mean gives the weighted values of the textural pattern seen in the individual printed layer image, which shall be designated as weighted texture in this study.

2.5 Normalized weighted mean calculation

Though the weighted mean gives a fair representation of the textural variations within the printed elements, the impact of brightness/illumination changes will influence the output. To eliminate the variabilities due to illumination, the mean and standard deviation of weighted mean values are computed for all the layers in the different printed elements separately. Then, each of the weighted HOG mean outputs of individual layer "i" of the printed element "j" is normalized using the following formula,

Normalized weighted mean for each layer image = $(x_{i,j} - \mu_j) / \sigma_j$

$x_{i,j}$ – HOG weighted mean of the individual layer "i" of printed element "j", μ_j – Mean value of all the individual layer's HOG weighted mean values of printed element "j", σ_j – Standard deviation value of all the individual layer's HOG weighted mean values of printed element "j". Normalized weighted mean values of the textural variation shall be identified as Normalized weighted texture in this study for ease of understanding.

2.6 Entropy value calculation

Another measure of textural variations generally used is information entropy by Shannon. It is used in this study, given by the formula,

Entropy = $-\sum P_i * \log_2 P_i$

Where, Pi – Ratio of the number of HOG pixel outputs for a threshold value "i" to the total number of pixels found (textural variations) in all the threshold value outputs. Entropy represents the distribution of pixel brightness/intensities within a given image. It indirectly measures the changes within a layer, like thickness variations due to the buildability properties of 3DP concrete material.

3 Results

3.1 Surface textural variation within a printed element – texture extraction

The individual layer images are processed using a CV-based HOG textural extraction algorithm for different threshold values. The output will be the number of pixels/points having textural variations beyond the specified threshold. For example, the HOG textural variation output of a few different threshold value outputs for layer L19 of printed element B is shown in Figure 5. Different positions/points in the image where textural variations exist are marked as black pixels. The output with a threshold value of 4 captures all the minor variations in the printed layers, leading to a higher density of black pixels. It captures both the minor variations within the printed layer and the major variations at the layer edges. In contrast, for the 128-threshold output, only the major textural variations that happen only at the layer edges and voids are captured. It is seen that the number of black pixels reduces and concentrates only on the layer edges as the threshold value increases.

32 different values for each layer image corresponding to different threshold values are shown in Figure 6. The outputs are for the bottom ten layers of the 3D-printed element B. From the results, it is evident that beyond the 128-threshold value, the output of the HOG algorithm is minimal. Hence the analysis was not done beyond the 128-threshold value.

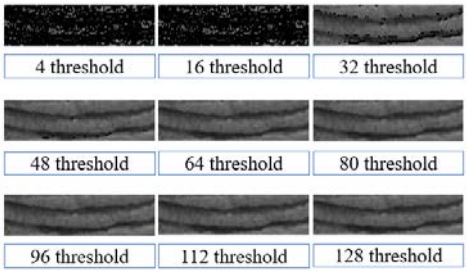

Figure 5 - HOG output for different threshold pixel values for individual layer - L19 of Element B

Layer Number	4 Threshold	8 Threshold	12 Threshold	16 Threshold	20 Threshold	24 Threshold	28 Threshold	32 Threshold	36 Threshold	40 Threshold	44 Threshold	48 Threshold	52 Threshold	56 Threshold	60 Threshold	64 Threshold	68 Threshold	72 Threshold	76 Threshold	80 Threshold	84 Threshold	88 Threshold	92 Threshold	96 Threshold	100 Threshold	104 Threshold	108 Threshold	112 Threshold	116 Threshold	120 Threshold	124 Threshold	128 Threshold
weight	1	2	3	4	5	6	7	8	9	10	11	12	13	14	15	16	17	18	19	20	21	22	23	24	25	26	27	28	29	30	31	32
L1	2340	1872	1437	1075	776	584	451	349	301	280	254	228	208	190	181	157	149	137	122	109	98	91	84	79	62	52	40	18	8	7	4	2
L2	2613	2058	1491	1027	685	419	247	147	103	66	39	27	17	14	14	12	12	12	11	9	9	8	6	6	4	4	2	2	2	2	0	0
L3	2643	1986	1442	1025	697	421	249	126	53	27	14	6	3	1	0	0	0	0	0	0	0	0	0	0	0	0	0	0	0	0	0	0
L4	2320	1617	1087	735	457	258	136	45	9	1	0	0	0	0	0	0	0	0	0	0	0	0	0	0	0	0	0	0	0	0	0	0
L5	2788	2039	1361	914	578	317	156	66	20	2	1	0	0	0	0	0	0	0	0	0	0	0	0	0	0	0	0	0	0	0	0	0
L6	2884	2111	1541	1104	748	456	256	114	47	17	10	3	1	1	0	0	0	0	0	0	0	0	0	0	0	0	0	0	0	0	0	0
L7	2538	1806	1246	858	563	357	191	78	32	13	5	0	0	0	0	0	0	0	0	0	0	0	0	0	0	0	0	0	0	0	0	0
L8	2111	1492	987	623	424	257	122	51	18	4	0	0	0	0	0	0	0	0	0	0	0	0	0	0	0	0	0	0	0	0	0	0
L9	2972	2152	1474	1049	741	470	261	147	72	34	14	6	1	0	0	0	0	0	0	0	0	0	0	0	0	0	0	0	0	0	0	0
L10	2967	2185	1575	1139	829	597	375	200	93	46	23	10	4	1	0	0	0	0	0	0	0	0	0	0	0	0	0	0	0	0	0	0

Figure 6 - HOG outputs for different threshold values for Element B (first ten layers)

3.1.1 Weighted mean variation – weighted texture calculation

The weighted texture is taken as a single measure of texture variation representation. A weightage of 32 is given to the 128-threshold output and reduced by one for every 4-pixel point reduction in the threshold value. Since the primary focus of this study is to identify layers with defects/voids, higher weightage is given to major textural variation outputs (128 threshold), and lesser weightage is given to minor textural variation outputs (4 threshold).

The outputs of the weighted texture for Element A and B are plotted in Figure 7. The weighted texture values obtained for Element B are higher than Element A. It is due to the presence of more voids and discontinuities in the printed layers. It confirms that Element A is a relatively good quality print in comparison to Element B.

3.1.2 Normalized weighted texture calculation

Further, a normalized weighted mean is computed from the weighted texture to evaluate the print quality, as shown in Figure 8. The standard deviation and mean of all the individual layer's HOG weighted texture output in

each printed element are calculated, and each data point is normalized in terms of mean and standard deviation within its printed element. It eliminates the influence of illumination and brightness variation during the different times of printing Elements A and B. The normalized values will be easy to compare and evaluate the effectiveness of the print quality. Also, this step eliminates the subjectivity in selecting weights for the weighted texture calculation. Making the technique more robust in terms of evaluation.

The results indicate that the normalized weighted texture values of Element B are generally higher than Element A. This means that the textural variations within the individual layers of Element B are higher than Element A. It indicates the presence of more granular texture and voids/defects in the individual layers. The evolution of normalized weighted texture for Elements A and B is explained in detail as follows,

Element A: From Figure 8, the normalized weighted texture values of the bottom layers of Element A are less than zero. The variations of values are also low, which can be directly correlated to the smooth textural finish of the bottom printed layers found in Figure 2. Beyond L20, higher value spikes were found (beyond the value of zero) in the normalized weighted texture values that can be directly related to the voids present in the individual layers of Element A. Beyond L20, some layers are not found to have any voids, which can be identified by the lower values of the normalized weighted texture. However, other layers having voids are characterized by higher normalized weighted texture values making the variation of values erratic. It can be visually understood that higher value spikes are found for individual layer elements having voids/deformities. And beyond L20, the concrete has lost significant value of moisture content requiring external interference to get good quality prints.

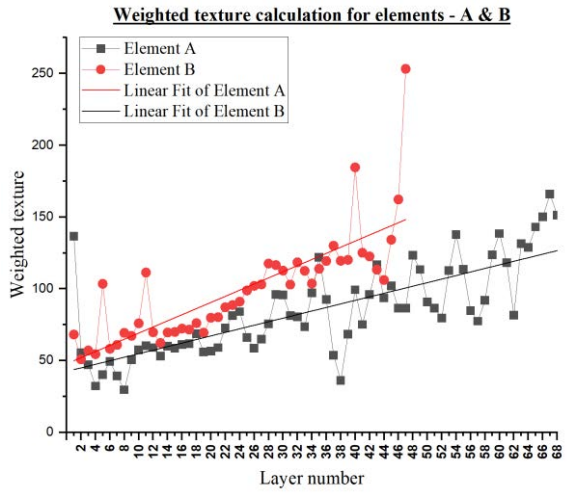

Figure 7 - Weighted texture output for the individual layer images of Element A and B

Element B: In contrast to Element A, Element B's normalized weighted texture values started to vary drastically and reach higher values (more than zero) in the initial layers. It can be correlated with voids/defects present in the initial few layers of Element B, as shown in Figure 3. But in the other bottom layers, due to sufficient workability, a smooth texture can be found, which is indicated by lower values of normalized weighted texture until L20. But, beyond L20, the values are always higher than zero and increasing, indicating the granular texture and the presence of voids/defects in every layer. Higher spikes in normalized weighted texture values beyond the value zero match with the layers having voids/deformities.

Further, the linear fit obtained on the normalized weighted texture values of elements A and B indicates a steep increase in the values for Element B compared to Element A. Hence, the slope of the linear fit of the normalized weighted texture values can also indicate the quality of the 3D printed elements.

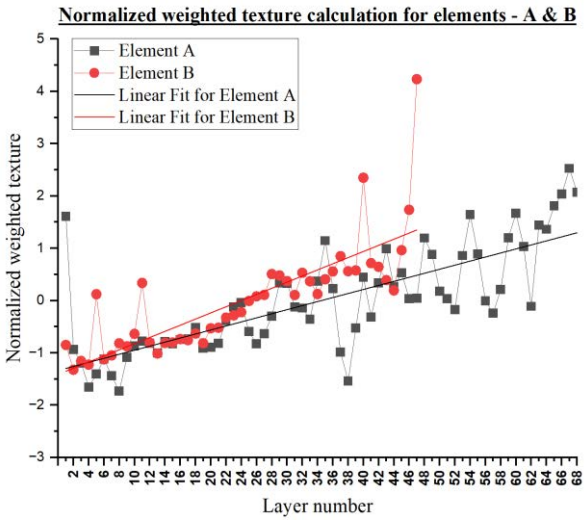

Figure 8 - Normalized weighted texture output of individual layer images of Element A and B

3.2 Temporal textural variation of a single printed layer

A temporal texture variations study is proposed to assess the buildability properties using surface texture analysis. To achieve this, temporal textural variation for a single layer of a printed element is extracted at different instances of printing to understand the variations happening on the individual layer due to the weight of the layers printed above it.

For a better-quality print, the thickness variations in the bottom layers due to the weight of the layers printed above should be minimum so that the final printed element will satisfy the dimensional and geometrical accuracy.

For this analysis, a video of the entire printing process is captured, and a single fixed crop window is selected for an individual layer of a printed element. The HOG textural variations are extracted at every instance a layer is printed above it. During this period, the target layer under study changes in dimension and textures. A single crop window consisting of layer L6 of Element A is considered, and images at different instances after the printing of every layer above it are shown in Figure 9. Similarly, crop windows were set for other layers like L7, and L8 of Element A and layers L21, L22, and L23 of Element B.

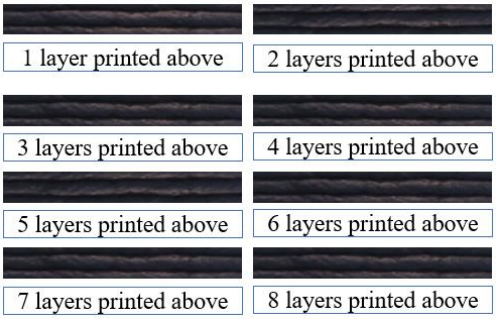

Figure 9 - Image of layer L6 of Element A after the number of layers printed above it

HOG textural values are extracted for each image for different threshold values, and the output is generated similar to that shown in Figure 6. To have a single output value, an entropy calculation is performed. The entropy values are obtained for the same layer at different instances after subsequent layers are printed above them. Entropy variations for the layers considered for analysis in Element A and Element B are plotted and shown in Figure 10 and Figure 11, respectively.

Element A – The entropy variation indicates the textural variations happening within the printed layer at that instance. First, the case of only one printed layer above the target layer is taken. The single layer above will not impart much weight on the layer below and will not cause a major reduction in the layer thickness. Hence, the printed layer is of its original printing height, and minor texture variations within the layers are predominant in the image. But as the number of layers printed above increases, the bottom layer compresses and makes the layer boundary more prominent visually. This results in the image consisting of predominantly dark pixels and causes a reduction in textural variations. The same is brought out in Figure 10, showing the reduction of entropy values as the number of printed layers increases. Beyond the four layers printed above, the thickness variation of the layer is reduced as the concrete reaches sufficient early strength to support the weight of the layers printed above, which is reflected with almost a flat curve in Figure 10.

Element B – In the case of Element B, it was difficult to study the temporal texture changes in the bottom layers as there were undulations and major voids. Hence, layers L21, L22, and L23 are considered where there are smaller voids. The layers' HOG entropy values are plotted in Figure 11. Layer L23 is found to exhibit similar trends, as shown in Figure 10. But in the case of layers L21 and L22, due to the presence of minor voids, the entropy values are found to vary drastically.

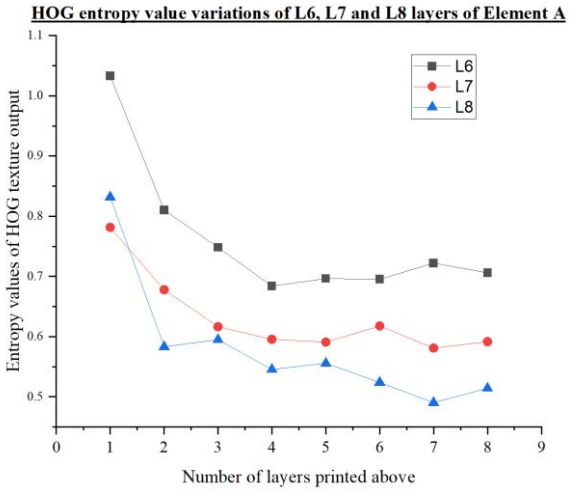

Figure 10 - Entropy value variations of HOG outputs for layers L6, L7, and L8 of Element A

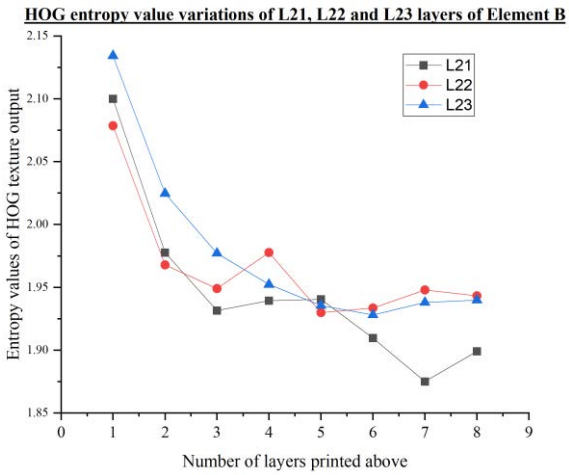

Figure 11 - Entropy HOG outputs for layers L21, L22, and L23 of Element B

4 Analysis and Discussion

4.1 Quality assessment of printed layers

From the previous section, it is plausible that the normalized weighted texture calculation is a valid representative of the textural variations within printed layers. Higher values were found for layers with

voids/defects, which can help classify the layers as bad quality.

Since the HOG texture extractor was designed to quantify textural variations in horizontal, vertical, and inclined directions, gradient variations in all directions are considered. The usage of different threshold values helps in capturing both minor and major textural variations, making it an end-to-end quality assessment technique for 3D printed elements.

This study analyzed two different elements printed at two different times and lighting conditions. The illumination changes and distance of the camera will have minimal effect on the results due to the following reasons: All the computations involve a relative comparison of output values obtained from the different layers of the same image. Further, a normalization technique is introduced, which allows for all the output values to be normalized in terms of the mean and standard deviation obtained over the entire image of the printed element. Due to this normalization procedure, the results are not very sensitive to the weighting scheme used for the weighted texture computation.

But in the case of off-site 3D printing, where the printing process is undertaken in a closed environment, a single trial 3D printed element can be printed and analyzed with the proposed technique to obtain the mean and standard deviation values. And using them, the quality of newly 3D printed elements during their printing can be assessed. Care should be taken to keep the camera position and printing material mix design constant.

Comparing the weighted texture values and the normalized weighted texture in Figure 7 and Figure 8, both graphs have a similar evolution of values (slope of the linear fit of values), matching the voids in the printed elements. Hence even the weighted texture values of the HOG feature extraction can be used as an effective quality assessment tool. But the normalized weighted texture measure is considered to significantly eliminate the impact of brightness/illumination changes, thereby making a robust controlled setup.

Overall, the normalized weighted texture values obtained from the HOG texture extractor prove to be a better-quality assessment metric for concrete 3D printed elements. It can further be used as a quality assessment tool for already printed layers after the printing process is completed.

4.2 A measure of workability and extrudability

The observed results from the computer vision model can be used to quantify the workability of the 3D printing concrete. The change in workability of the mix used for printing Element A was studied and found to be reducing with time, as shown in Figure 12 [10]. A flow table test was conducted to quantify the workability change with time for the material matching the mix used for this study, LC2-MS-0.6SP (Limestone Calcined Clay mix with Manufacture Sand and Super Plasticizer).

It is to be noted that the spread diameter from the flow table test keeps on reducing every half an hour, indicating a reduction in workability.

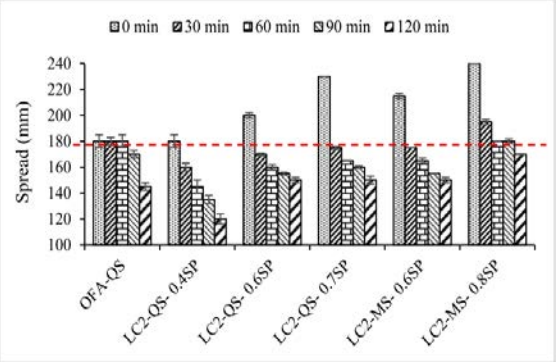

Figure 12 - Evolution of workability of 3DP concrete with time-based on flow table test [10]

Characterization of workability for every 5 to 10 minutes is not considered in the scope of this study, but the graph indicates the reduction in workability with time. There is a reduction in workability with time, whereas there is an increase in the normalized weighted texture values from HOG. Hence an inverse correlation can be obtained, which helps in indirect non-intrusive quantification of workability. The workability can be directly related to the extrudability properties of the 3DP concrete. Hence the developed methodology can be used to indirectly quantify the extrudability and workability properties of concrete 3D printing.

4.3 An Assessment of Buildability Properties

In section 3.2, HOG entropy values are found to be high in the initial instance when only one layer is printed above it. But as the number of layers printed above increases, the bottom layer has sufficient time to gain early strength. This phenomenon was captured in this analysis; the HOG entropy values are found to stabilize and flatten after the printing of four layers above any target layer. But in the case of layers L21 and L22 of element B, the HOG textural variations are not found to stabilize even after the printing of four layers above it. It is due to the presence of minor voids in the layers. Hence, if the HOG textural variations are not found to stabilize within a few printed layers, then it indicates the presence of voids or the failure of buildability properties. A detailed study of buckling is outside the scope of this study. The developed methodology is intended to provide early indications of buildability issues. This study can be used to monitor and assess the buildability properties of 3DP concrete during the printing process.

5 Conclusion

A quality control and assessment technique for concrete 3D printed elements based on computer vision has been developed in this study. Using continuous monitoring, several possible defects leading to wastage in terms of cost, materials, and time are avoided, reinforcing the sustainability aspects of concrete 3D printing technology. The variations in the surface texture of the concrete due to the reduction in workability or moisture content are analyzed using 2D images taken through a camera. The main contribution of this study is the introduction of a new algorithm for texture extraction based on the concept of Histogram of Oriented Gradients (HOG). This algorithm uses multiple threshold levels to capture minor and major textural variations. Also, the normalized weighted texture value of the distribution is found to be an appropriate metric to quantify the textural variations. This metric is found to have higher values for layers having voids. Also, the values increase as the granularity of the layers increases resulting in a reduction in workability. Further, a temporal changes study is also conducted for an individual layer to understand the variations within the layer due to the buildability properties. The significant conclusions obtained from this study are as follows,

- A continuous, non-intrusive method to monitor the temporal changes in the extrudability properties of 3D printing concrete has been achieved.
- The newly developed method is less sensitive to variations in illuminance levels. The normalized weighted texture minimizes the influence of differential brightness/illumination changes.
- Results show that the defects and voids present in the 3DP layers can be autonomously detected.
- An inverse correlation is observed between the normalized weighted texture value and the workability over time. This means that the workability properties of concrete can be indirectly quantified using texture data.
- Temporal textural variation study helps in indirectly assessing the buildability properties. The changes in layer thickness can be correlated to the changes in the textural variations.

Results prove the feasibility of using computer vision-based texture extraction methods for quality monitoring of 3D printed elements. Further, the quality assessment obtained can be used as feedback to the printing system to control the printing parameters like extrusion and printing speed to achieve a better-quality print. Increasing the extrusion speed will help in making the concrete material shear and flow continuously without voids and discontinuities. As a result, a change in the normalized weighted texture value can be used as feedback to the printing system for taking corrective actions to avoid material wastage and achieve high-quality output. The study opens many opportunities to extract useful information from non-intrusive based sensor data collected to help the sustainability aspects of 3D printing technology.

References

[1] M. Hoffmann, S. Skibicki, M. Techman, Automation in the Construction of a 3D-Printed Concrete Wall with the Use of a Lintel Gripper, (2020). https://doi.org/10.3390/ma13081800.

[2] R. Buswell, P. Kinnell, J. Xu, N. Hack, H. Kloft, M. Maboudi, M. Gerke, P. Massin, G. Grasser, R. Wolfs, F. Bos, Inspection Methods for 3D Concrete Printing, RILEM Bookseries. 28 (2020) 790–803. https://doi.org/10.1007/978-3-030-49916-7_78.

[3] A. Kazemian, X. Yuan, O. Davtalab, B. Khoshnevis, Automation in Construction Computer vision for real-time extrusion quality monitoring and control in robotic construction, Autom Constr. 101 (2019) 92–98. ttps://doi.org/10.1016/j.autcon.2019.01.022.

[4] Y. Zhang, Y. Zhang, W. She, L. Yang, G. Liu, Y. Yang, Rheological and harden properties of the high-thixotropy 3D printing concrete, Constr Build Mater. 201 (2019) 278–285. https://doi.org/10.1016/j.conbuildmat.2018.12.061.

[5] S. Ahmed, S. Yehia, Evaluation of Workability and Structuration Rate of Locally Developed 3D Printing Concrete Using Conventional Methods, Materials. 15 (2022). https://doi.org/10.3390/ma15031243.

[6] S. Senthilnathan, B. Raphael, Using Computer Vision for Monitoring the Quality of 3D-Printed Concrete Structures, Sustainability (Switzerland). 14 (2022). https://doi.org/10.3390/su142315682.

[7] A. Oleff, B. Küster, M. Stonis, L. Overmeyer, Process monitoring for material extrusion additive manufacturing: a state-of-the-art review, Progress in Additive Manufacturing. (2021) 23–27. https://doi.org/10.1007/s40964-021-00192-4.

[8] O. Davtalab, A. Kazemian, X. Yuan, B. Khoshnevis, Automated inspection in robotic additive manufacturing using deep learning for layer deformation detection, J Intell Manuf. (2020). https://doi.org/10.1007/s10845-020-01684-w.

[9] R. Rill-García, E. Dokladalova, P. Dokládal, J.-F. Caron, R. Mesnil, P. Margerit, M. Charrier, Inline monitoring of 3D concrete printing using computer vision, Addit Manuf. 60 (2022) 103175. https://doi.org/10.1016/j.addma.2022.103175.

[10] B. Shantanu, J. Smrati, S. Manu, Criticality of binder-aggregate interaction for buildability of 3D printed concrete containing limestone calcined clay, Cem Concr Compos. 136 (2023) 104853. https://doi.org/10.1016/j.cemconcomp.2022.104853.

[11] L. Armi, S. Fekri-Ershad, Texture image analysis and texture classification methods - A review, 2 (2019) 1–29. http://arxiv.org/abs/1904.06554.